Microscopic Deformation of Tungsten Surfaces by High Energy and High Flux Helium/Hydrogen Particle Bombardment with Short Pulses

Masayuki TOKITANI, Naoaki YOSHIDA[1)], Kazutoshi TOKUNAGA[1)], Hajime SAKAKITA[2)], Satoru KIYAMA[2)], Haruhisa KOGUCHI[2)], Yoichi HIRANO[2)] and Suguru MASUZAKI

National Institute for Fusion Science, Toki, Gifu 509-5292, Japan
[1)]*Research Institute for Applied Mechanics, Kyushu University, Kasuga, Fukuoka 816-8580, Japan*
[2)]*National Institute of Advanced Industrial Science and Technology (AIST), Tsukuba, Ibaraki 305-8568, Japan*

(Received 24 August 2009 / Accepted 14 December 2009)

The neutral beam injection facility in the National Institute of Advanced Industrial Science and Technology was used to irradiate a polycrystalline tungsten specimen with high energy and high flux helium and hydrogen particles. The incidence energy and flux of the beam shot were 25 keV and 8.8×10^{22} particles/m^{2}s, respectively. The duration of each shot was approximately 30 ms, with 6 min intervals between each shot. Surface temperatures over 1800 K were attained. In the two cases of helium irradiation, total fluence of either 1.5×10^{22} He/m^2 or 4.0×10^{22} He/m^2 was selected. In the former case, large sized blisters with diameter of 500 nm were densely observed. While, the latter case, the blisters were disappeared and fine nanobranch structures appeared instead. Cross-sectional observations using a transmission electron microscope (TEM) with the focused ion beam (FIB) technique were performed. According to the TEM image, after irradiation with a beam shot of total fluence 4.0×10^{22} He/m^2, there were very dense fine helium bubbles in the tungsten of sizes 1-50 nm. As the helium bubbles grew the density of the tungsten matrix drastically decreased as a result of void swelling. These effects were not seen in hydrogen irradiation case.

Keywords: hydrogen, high energy, high fluence, tungsten, nanoscale structure, blister, bubble

DOI: 10.1585/pfr.5.012

1. Introduction

Tungsten is a candidate for divertor armor material in the International Thermonuclear Experimental Reactor (ITER). In ITER conditions, strong erosion and radiation damage on the divertor surface, caused by high heat and particle loading as a result of disruptions and edge localized modes (ELMs), are critical issues to consider in the preparation of divertor armors of good thermal and mechanical properties. To this end, in previous studies heat loading tests made by electron beam machines [1, 2] and particle loading tests made by plasma machines [3, 4] were performed. However, evaluation of synergistic loading effects of high heat and helium/hydrogen with short pulses is necessary for confirming the reliability of tungsten armor tiles. Although some experiments on this topic were performed [5–7], they mainly focused on the microscale or macroscale phenomena. In order to understand the mechanism causing the damage evolution, we must focus on nanoscale structures.

Helium irradiation effects with high heat loads should specially be noted because once helium is injected into metals, it causes serious damaging effects. Furthermore, helium injected into metals is not easily released until the temperature is high because of its strong interaction with lattice defects such as vacancies and dislocation loops [8]. Tungsten irradiation tests by divertor plasmas in the large helical device (LHD) indicated that synergistic effects of heat and helium/hydrogen particle load lead to damage and erosion of the tungsten surface [9, 10].

Therefore, the helium or hydrogen irradiation experiment with high heat loading is important not only for elucidation of the damage evolution but also safety assessment of tungsten walls for fusion devices. In this study, high energy and high flux helium and hydrogen particles irradiated polycrystalline tungsten specimens at the neutral beam injection (NBI) facility in the National Institute of Advanced Industrial Science and Technology (AIST). After the exposure, nanoscale deformation and damage evolution were investigated using focused ion beam (FIB) fabrication and transmission electron microscope (TEM) observations. In order to investigate further the effect of bombardment of tungsten by helium and hydrogen particles, optical reflectivity was measured using a spectrophotometer for the wavelengths in the range 190-2500 nm. The correlation between optical reflectance and radiation damage evolution found in this study will suggest that measure-

author's e-mail: tokitani.masayuki@LHD.nifs.ac.jp

ments of optical reflectivity may be used to predict the radiation damage caused by heat and particle loads.

This study is a fundamental research focused on the nanoscale damage evolution in tungsten due to the energetic particle bombardment under high heat loading.

2. Experimental Procedures

2.1 Beam conditions and setups

The high-power-density NBI system with strong focusing characteristics was developed at AIST for heating profile control of the reversed field pinch (RFP) plasma [11]. The typical beam energy and duration of each shot are 25 keV and 30 ms, respectively, and its maximum current is 90 A. The power density of the beam becomes more than 1 GW/m^2 at the focal region. In the present experiments, gas puffing into the neutralization cell was not conducted. This ion beam system has many applications, including its use as a beam source for alpha particle measurements in ITER and its use in irradiation tests of materials [12].

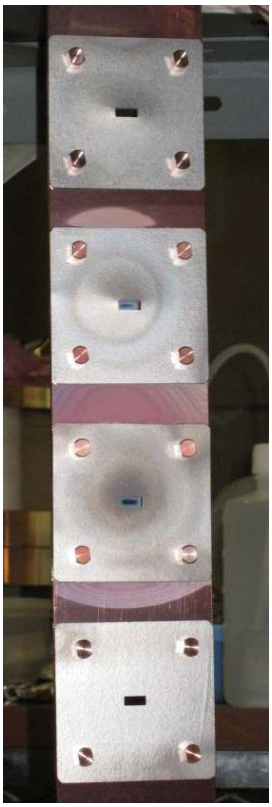

Fig. 1 Specimen stage.

Table 1 The approximate length of the irradiation pulse times the number of shots (pulses), total irradiation time, power density, and total fluence for each irradiation pattern.

	Pulse x shot	Total Irr. time	Power density	Fluence
He	~30 ms x 7 shot	171 ms	300 MW/m^2	1.5x10^{22} He/m^2
	~30 ms x 16 shot	461 ms	300 MW/m^2	4.0x10^{22} He/m^2
H	~30 ms x 5 shot	146 ms	300 MW/m^2	1.3x10^{22} H/m^2
He+H	~30 ms x 15 shot	447 ms	300 MW/m^2	3.9x10^{22} He+H/m^2

High purity (~99.95%) powder metallurgy (PM) tungsten specimens of 10 × 5 × 1 mm^3 were mounted at the focus point of the beam using a special specimen stage as shown in Fig. 1. Then these specimens were irradiated with helium, hydrogen and He + H beams. The incidence energy and beam current were fixed at 25 keV and 40 A, respectively. The diameter of the focused beam was estimated to be ~60 mm, and the power density and flux were 300 MW/m^2 and 8.8 × 10^{22} particles/m^{2}s. The duration time of each shot was 30 ms with a 6 min interval between each shot. Total irradiation time and fluence of each irradiation pattern were summarized in Table 1. In the case of He+H irradiation, helium beam ratio is less than 80% compared with hydrogen beams. Although the surface temperature was measured using an optical pyrometer and thermocouples embedded just behind the specimen, unfortunately, its exact value was impossible to determine. The expected surface temperature determined using the optical pyrometer was approximately 1800 K.

2.2 Material analysis

After the exposure, surface morphology was analyzed using scanning electron microscope (SEM). In order to clarify the depth distribution of nanoscale damages, cross-sectional microscopic observations were conducted using FIB fabrication and TEM observations.

Furthermore, to investigate the effect of bombardment of helium and hydrogen particles on optical reflectivity, change of optical reflectivity was measured by means of spectrophotometer.

3. Results and Discussions

3.1 Surface morphology

Figure 2 shows surface photos and SEM images of tungsten specimens after irradiation by helium, hydrogen, and He + H beams. The irradiated area on the specimens was about 8 × 3 mm^2. In the cases of helium irradiation, total fluence was selected 2 patterns of 1.5 × 10^{22} He/m^2 and 4.0 × 10^{22} He/m^2. In the former pattern, the surface color changed to gray, and large blisters with the diameter of 500 nm were densely observed. While, the latter pattern, the blisters disappeared as a result of sputtering erosion, and the surface became smoother in the low magnification SEM image; however, in the high magnification SEM image, fine nanobranch structures appeared instead of blisters. These fine nanobranch structures may affect the degradation of optical reflectivity in the visible wavelength, actually, the surface color turned to dark brown. Section 3.3 discusses optical reflectivity in detail.

In the case of hydrogen irradiation, although intensive

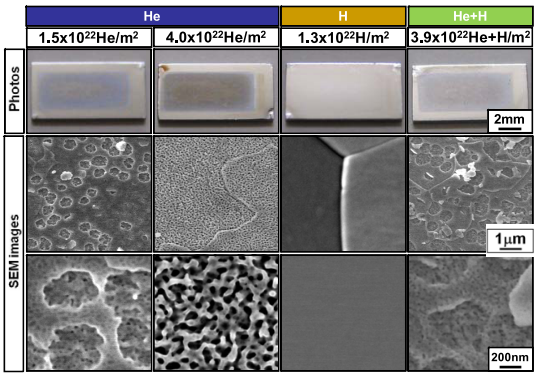

Fig. 2 Surface photos and SEM images of tungsten specimens after irradiation by He, H, and He + H beams.

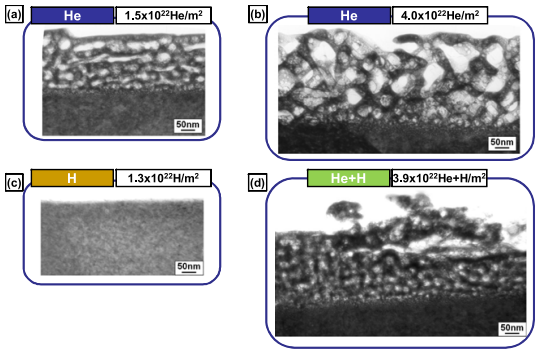

Fig. 3 Cross-sectional TEM images of tungsten specimens after beam irradiation with (a) 1.5×10^{22} He/m^2, (b) 4.0×10^{22} He/m^2, (c) 1.3×10^{22} H/m^2 and (d) 3.9×10^{22} He+H/m^2.

grain growth was observed, there was no sign of remarkable deformation. These discrepancies of the surface deformation between helium and hydrogen seem to be the result of the difference in their behaviors inside materials. In the case of helium, surface modifications are considered to be due to the formation, coalescence, and migration of helium bubbles near the surface during the pulse high heat loading. However, hydrogen irradiation does not cause these effects. It is known that retention of hydrogen isotopes in tungsten is low in general, and this is one of the advantages of this material [13].

Furthermore, in the case of simultaneous irradiation by He and H, surface morphology was quite similar to the lower fluence case of helium irradiation (1.5×10^{22} He/m^2). This means that damage evolution of the surface does not depend on the hydrogen fluence.

3.2 Depth distribution of nanoscale damages

In order to clarify the depth distribution of radiation damages, we needed cross-sectional images of the subsurface region at the nanometer level. FIB fabrication was used to obtain cross-sectional samples for these nanometer observations. Figures 3 (a)-(d) show TEM images of the four exposure patterns listed in Table 1.

In the case of lower helium irradiation (case a), dense helium bubbles with sizes 1-50 nm were observed up to a depth of 200 nm. It is notable that many of the bubbles were larger than 20 nm, and some of them had oddly shaped images like a three dimensional ellipse or even a gourd. This indicates that the bubbles grew by coalescence as the temperature abruptly increased, and the non-equilibrium shapes were "frozen" by rapid cool-down after the termination of the beam pulses. Although the average penetration depth of 25 keV-He in tungsten was estimated to be about 60 nm by TRIM-code, the heavily damaged region was much deeper than this. This discrepancy may have been caused not only by diffusion of injected helium atoms into the deeper region, but also by void swelling of the surface.

In the case of higher helium irradiation (case b), dense helium bubbles with sizes 1-100 nm were observed with nanobranch structures, and many of the bubbles were larger than 50 nm (much larger than that of lower helium irradiation). Thus the density of the tungsten matrix was drastically decreased by void swelling, and its depth distribution was over 300 nm. On the surface of this specimen (shown in Fig. 2), the blisters lid observed in case of low helium irradiation disappeared, and this was caused by the sputtering erosion and microscopically localized melting of the blisters. In the high helium irradiation stage, accumulation of helium atoms by implantation in the matrix, loss by sputtering erosion, and exfoliation of blisters were balanced. Therefore, if helium were continuously irradiated, nanobranch structures would not disappear.

In the case of hydrogen irradiation (case c), nanoscale damages scarcely formed, and it corresponded to the surface observation result shown in Fig. 2. It is considered that hydrogen irradiation could not cause serious radiation damage even at the high energy and high flux condition, because hydrogen atoms scarcely interact with lattice defects. In contrast, helium irradiation causes serious radiation damage because once helium is injected into metals, it strongly interacts with lattice defects such as vacancies and dislocation loops.

In the case of simultaneous irradiation of hydrogen and helium, (case d), the size, density, and depth distribution of helium bubbles were very similar to the case of low helium fluence (case a). As mentioned above, damage evolution does not depend on the hydrogen fluence. Thus, helium irradiation effects in tungsten indicate that serious consideration should be given to the surface erosion of tungsten walls by helium irradiation.

3.3 Optical reflectivity

Figure 4 (a)-(d) shows the optical reflectivity of tungsten specimens after the beam irradiation. The reflectivity of the virgin specimen is also plotted for reference. It is

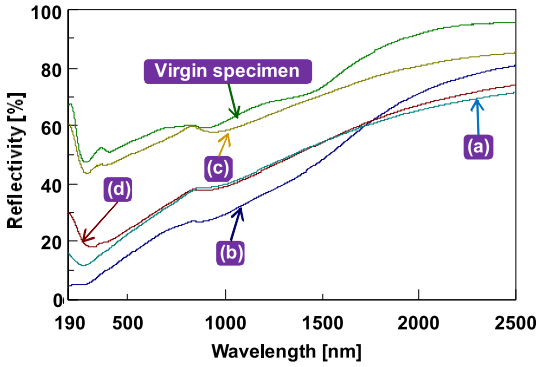

Fig. 4 Optical reflectivity of tungsten specimens before beam irradiation (virgin specimen) and after beam irradiation with (a) 1.5×10^{22} He/m^2, (b) 4.0×10^{22} He/m^2, (c) 1.3×10^{22} H/m^2 and (d) 3.9×10^{22} He+H/m^2.

clear that a strong reduction in reflectivity has occurred in all of the helium irradiation cases (a, b, and d). In particular, the reduction of reflectivity around 500 nm is remarkable. Referring to our previous study [14], the reduction of optical reflectivity is most likely due to multiple scattering of light by dense helium bubbles in the sub-surface region. In cases (a) and (d), the spectrum of the reflectivity is very similar throughout the measured wavelength range of 190-2500 nm. The optical reflectivity may depend on both the surface morphology and the depth distribution of nanoscale damage, because surface morphology and depth distribution were similar in Fig. 2 and Fig. 3. On the other hand, for the high helium irradiation case of (b), although drastic degradation with ~40% decrease in the optical reflectivity from the virgin specimen occurred in the short wavelength range (190-1000 nm), there is less degradation and only a ~20% decrease in its optical reflectivity in the long wavelength range. We consider the following mechanisms for this phenomenon. The overall reduction in reflectivity was probably due to surface roughening and fine bubble formation. The drastic degradation at short wavelength range (190-1000 nm) nm was caused by the formation of nanobranch structures with nanoscale helium bubbles as shown in Fig. 3 (b). The recovery of higher reflectivity at long wavelength range (2000-2500 nm) was caused by the smoothening of the surface due to the progress of the sputtering erosion as shown in Fig. 2. However, it is necessary to consider in future work what causes the reduction in reflectivity at the middle wavelengths around 1500 nm.

In the case of hydrogen irradiation (c), although slight degradation with ~15% decrease in optical reflectivity was observed in the long wavelength range (1500-2500 nm), remarkable degradation was not confirmed at most wavelengths. We note that the effect of helium bombardment is much higher than that of hydrogen bombardment. This result is important for the design and operation of plasma diagnostics using tungsten as a first mirror.

4. Summary

The high-power-density NBI facility at AIST was used to shoot high energy and high flux beams of helium and hydrogen particles at tungsten specimens. Then nanoscale deformations and damage evolution of the tungsten specimens were investigated.

In the case of helium irradiation, very dense fine helium bubbles of the size 1-100 nm were observed, and as the helium bubbles grew, the density of the tungsten matrix decreased drastically by void swelling. In the hydrogen irradiation case, these damages were not observed.

We investigated the effect that bombarding tungsten specimens with helium and hydrogen particles had on optical reflectivity. In the hydrogen irradiation case, reflectivity scarcely changed before and after irradiation. However, a reduction in the reflectivity was observed in both helium irradiation cases: a remarkable drop in reflectivity was observed in the wavelength of near 500 nm. This reduction of optical reflectivity is likely to be due to the multiple scattering of light by helium bubbles in the sub-surface region.

High energy and high flux helium irradiation effects on tungsten indicate that serious consideration should be given to the surface erosion of tungsten walls by helium. Furthermore, if tungsten is used as a first mirror, its design and operation will also require serious consideration.

Acknowledgements

A part of this study was financially supported by the Budget for Nuclear Research of the Ministry of Education, Culture, Sports, Science and Technology of Japan, based on the screening and counseling of the Atomic Energy Commission.

[1] K. Tokunaga *et al.*, Fusion Eng. Des. **81**, 133 (2006).
[2] X. Liu *et al.*, J. Nucl. Mater. **329-333**, 687 (2004).
[3] D. Nishijima *et al.*, Mater. Trans. **46**, No.3, 561 (2005).
[4] D. Nishijima *et al.*, J. Nucl. Mater. **313-316**, 97 (2003).
[5] K. Tokunaga *et al.*, J. Nucl. Mater. **307-311**, 130 (2002).
[6] K. Tokunaga *et al.*, J. Nucl. Mater. **329-333**, 757 (2004).
[7] S. Tamura *et al.*, J. Nucl. Mater. **337-339**, 1043 (2005).
[8] T. Baba *et al.*, Mater. Trans. **46**, No.3, 565 (2005).
[9] M. Tokitani *et al.*, J. Nucl. Mater. **337-339**, 937 (2005).
[10] M. Tokitani *et al.*, J. Nucl. Mater. **363-365**, 443 (2007).
[11] H. Sakakita *et al.*, Proc. of IAEA Fusion energy conf. 2006, FT/P5-2.
[12] M. Sasao *et al.*, Rev. Sci. Instrum. **77**, 10F130 (2006),
[13] N. Yoshida and Y. Hirooka, J. Nucl. Mater. **258-263**, 173 (1998).
[14] A. Ebihara *et al.*, J. Nucl. Mater. **363-365**, 1195 (2007).